Available online at www.sciencedirect.com

ScienceDirect

www.elsevier.com/locate/jes

JES JOURNAL OF ENVIRONMENTAL SCIENCES

www.jesc.ac.cn

Phenotype and metabolism alterations in PCB-degrading *Rhodococcus biphenylivorans* TG9^T under acid stress

Aili Li[1], *Jiahui Fan*[1], *Yangyang Jia*[1], *Xianjin Tang*[2], *Jingwen Chen*[1], *Chaofeng Shen*[1,*]

[1] *Department of Environmental Engineering, College of Environmental and Resource Sciences, Zhejiang University, Hangzhou 310058, China*

[2] *MOE Key Lab of Environmental Remediation and Ecosystem Health, College of Environmental and Resource Sciences, Zhejiang University, Hangzhou 310058, China*

ARTICLE INFO

Article history:
Received 22 February 2022
Revised 11 May 2022
Accepted 12 May 2022
Available online 21 May 2022

Keywords:
Environmental acidification
Rhodococcus biphenylivorans
Contaminant degradation
Phenotypic response
Transcription analysis
Metabolism pathway
Mechanism model

ABSTRACT

Environmental acidification impairs microorganism diversity and their functions on substance transformation. *Rhodococcus* is a ubiquitously distributed genus for contaminant detoxification in the environment, and it can also adapt a certain range of pH. This work interpreted the acid responses from both phenotype and metabolism in strain *Rhodococcus biphenylivorans* TG9^T (TG9) induced at pH 3. The phenotype alterations were described with the number of culturable and viable cells, intracellular ATP concentrations, cell shape and entocyte, degradation efficiency of polychlorinated biphenyl (PCB) 31 and biphenyl. The number of culturable cells maintained rather stable within the first 10 days, even though the other phenotypes had noticeable alterations, indicating that TG9 possesses certain capacities to survive under acid stress. The metabolism responses were interpreted based on transcription analyses with four treatments including log phase (LP), acid-induced (PER), early recovery after removing acid (RE) and later recovery (REL). With the overview on the expression regulations among the 4 treatments, the RE sample presented more upregulated and less downregulated genes, suggesting that its metabolism was somehow more active after recovering from acid stress. In addition, the response mechanism was interpreted on 10 individual metabolism pathways mainly covering protein modification, antioxidation, antipermeability, H^+ consumption, neutralization and extrusion. Furthermore, the transcription variations were verified with RT-qPCR on 8 genes with 24-hr, 48-hr and 72-hr acid treatment. Taken together, TG9 possesses comprehensive metabolism strategies defending against acid stress. Consequently, a model was built to provide an integrate insight to understand the acid resistance/tolerance metabolisms in microorganisms.

Introduction

Since the last decades, abundant fossil fuels and mineral fertilizer consumed have dramatically increased the amount of

* Corresponding author.
E-mail: ysxzt@zju.edu.cn (C. Shen).

https://doi.org/10.1016/j.jes.2022.05.016
1001-0742/

CO_x, NO_x and SO_x in environmental compartments, which cause the acidification of soil and water bodies (Martins et al., 2019; Guo et al., 2010; Doney et al., 2020). In addition, due to the rapid upgrade of electronic products, informal electrical and electronic waste recycling is another key environmental acid source in developing countries. Meanwhile, acid mine drainage is also a contribution to environmental acidification resulting from oxidation and biooxidation of sulfur minerals such as pyrite (Edraki et al., 2005; Favas et al., 2016). Accompanied with these inorganic acid sources, a large amount of organics and heavy metals can also enter the environment, accelerating environmental degradation (Ge et al., 2020; Arya et al., 2021; Huang et al., 2021). Microbial communities play an indispensable role in contaminant detoxification and substance transformation. However, it has been found that acidification can affect nutrient cycling, organism biomass, taxonomic diversities and structures in both soil and aqueous environment, and then influences the ecosystem and human health (Meng et al., 2019; Yun et al., 2016). In particular, most microorganisms are rather sensitive to pH variations in their media, and acidified pH can lower their viability, metabolic activities and environmental functions (Zhang et al., 2015; Shen et al., 2018). Differently, some species possess certain coordinating systems in response to acid stress, such as *Escherichia coli, Salmonella enterica, Shigella* spp., *Vibrio cholera* and so on (Merrell and Camilli, 2002; Liu et al., 2015; Hu et al., 2020; Guan and Liu, 2020).

The genus *Rhodococcus* is ubiquitously distributed in environment media and dozens of species have been discovered and isolated (Jones and Goodfellow, 2015; Bell et al., 1998). They have rather strong capability to survive in certain range of salinity, temperature, pH, desiccation, osmosis and nutrient deficiency (Carvalho and Fonseca, 2005; LeBlanc et al., 2008; Suyal et al., 2019 . It has been recognized that they are of great importance for environmental remediation including degradation of recalcitrant pollutants, accumulation and reduction of heavy metals, desulfurization and denitrification of fossil fuels (Inoue et al., 2020; Zhang et al., 2019; Dobrowolski et al., 2017; Maass et al., 2015). Due to its strong environmental adaptabilities and comprehensive catabolic pathways, it is worthwhile to explore the potential of environmental remediation by *Rhodococcus*, especially under unfavorable conditions. As mentioned above, environmental acidification has been an increasingly concerned issue and microorganisms are critical agents in environmental compartments, hence it is necessary to understand their physiological characteristics and metabolic mechanisms under acidified conditions.

The first barrier microorganisms employ for acid resistance is to reduce proton influx into cytoplasm through plasma membrane by restricting membrane permeability or modulating the size of membrane channels (Sohlenkamp, 2017). This adaption involves the modifications of the composition and distribution of fatty acids, which have been found in *Escherichia. coli, Sccharomyces cerevisiae* and *Zygosaccharomyces bailii* (Chang and Cronan, 1999; Lindberg et al., 2013; Guo et al., 2018). In addition to the repression of proton entry, microorganisms also possess the ability to promote proton efflux in the electron transport chain of oxidative phosphorylation assisted with ATP consumption (Sun, 2016). This activity is especially observed in acidophiles for maintaining their intracellular pH, such as *Acidithiobacillus thiooxidans, Acidithiobacillus caldus* (Feng et al., 2015; Mangold et al., 2013). Besides, many microorganisms can neutralize excessive cytoplasmic protons with ammonia released from the transformation of urea or amino acids, or consume the protons via glutamate decarboxylation (Zhou and Fey, 2020; Lyu et al., 2018). Combining the acid resistance systems, microorganisms also have metabolic regulations for acid tolerance, including the repair of DNA and proteins and the increase of energy metabolism (Guan et al., 2014; Chakraborty et al., 2017). Different species, however, mostly have their specific response to facilitate survival under acid stress.

So far, acid resistance and tolerance mechanisms have been mostly studied on some specific genera directly related to industrial production or human health, such as *Lactococcus* (Zhu et al., 2019), *Lactobacillus* (Bang et al., 2018), *Escherichia* (Zhang et al., 2021), *Saccharomuces* (Palma et al., 2018), *Streptococcus* (Domínguez-Ramírez et al., 2020), *Propionibacterium* (Jan et al., 2001), *Salmonella* (Kenney, 2019) and so on. In addition, as we found that the research about acid stress on *Rhodococcus* has only been conducted on pathogen *Rhodococcus equi*, and the work was just focused on cell survivability and the expression regulations of *vap* genes (Benoit et al., 2001; Benoit et al., 2000). As mentioned above, acidification has been a globally concerned environmental issue, so it is necessary to pay attention to the acid effects on environmental microbiomes, especially the ones that are important for substance transformation and contamination bioremediation. In this study, it is focused on the phenotype and metabolism responses of the environmental strain *Rhodococcus biphenylivorans* $TG9^T$ (TG9) under acid stress. The phenotype was described with cell survivability, intracellular ATP concentrations, morphologies and contaminant degradation efficiency, and the metabolism responses were explained with gene expression regulations based on transcription analyses. Consequently, a metabolism model was built to present the potential surviving strategies under acid stress in TG9, which could also provide a reference for acid resistance and tolerance in other microorganisms.

1. Material and methods

1.1. Strain cultivation and induction

TG9 is a Gram-positive, aerobic, rod-shape actinobacterial strain, isolated from river sediment in Taizhou city, China (Su et al., 2015). The strain cells were cultivated in Lennox Broth (LB) (ThermoFisher Scientific, USA) liquid culture at 30°C with 180 r/min until log phase with an optical density at 600 nm (OD_{600}) of 1.2. The log-phase culture was adjusted to pH 3 with HCl and divided into four conical flasks as four biological replicates for acidification induction, and then incubated in the shaker.

1.2. Cell counting

The number of total cells and viable cells were counted using flow cytometry (BD FACSMelody, New Zealand). Using

CountBright™ absolute counting beads (Thermofisher Scientific, USA) as a reference, the number of total cells was calculated based on the number of the beads added to the test samples. Since the viable cells can reduce the stain 5-cyano-2,3-ditolyl tetrazolium chloride (CTC) (Biotium, USA) into an insoluble, red fluorescent formazan product via respiration electron transport chain, the viable cells can be differentiated and semi-quantified with the stain. The harvested cells were washed twice and resuspended in saline, and 10 μL of CTC was added to 500 μL of each sample, incubating 1.5 hr at 30°C in the dark for the reduction reaction. Before tested with flow cytometry, 50 μL of counting beads was added to each sample for cell quantification. In addition, the number of the culturable cells was counted with the number of colony forming units (CFU) using LB agar plates which were incubated at 30°C for 48 hr. The quantification limit of the culturability is 1 CFU/2 mL. The determination and quantification were performed with 4 biological replicates.

1.3. *Determination of intracellular ATP content*

The intracellular ATP concentrations were determined with ATP Bioluminescence Assay Kit (Beyotime Biotechnology, S0026, China) following its operation instructions. Gathered cells were lysed with 200 μL of lysis solution and 20 μL of the lysed supernatant was mixed with 100 μL of dilution buffer containing luciferase for luminance detection. ATP content was calculated with standard curve and blank control. The determination was performed including 4 biological replicates × 3 technical replicates, the error bars of the results were calculated based on the 4 biological replicates.

1.4. *Morphology observation*

The log-phase cells and the acid-induced cells (induction until no culturability on day 19) were sampled and treated for morphology observation using scanning electron microscope (SEM) (Hitachi Model SU-8010, Japan) and transmission electron microscope (TEM) (Hitachi Model H-7650, Japan). The gathered cells were first fixed in 2.5% glutaraldehyde solution at 4°C for more than 4 hr and then washed three times in PBS. Subsequently, the cells were further fixed in 1% OsO_4 for 1.5 hr and washed three times in PBS.

For SEM observation, the fixed specimens were first dehydrated with different concentration gradients of ethanol (30%, 50%, 70%, 80%, 90%, 95% and 100%), and then stored in 100% ethanol. Furthermore, the specimens were dehydrated with Hitachi Model HCP-2 critical point dryer (Japan). Consequently, they were coated with gold-palladium with Hitachi Model E-1010 ion sputter (Japan) for 5 min, and observed using SEM.

For TEM observation, the fixed specimens were first dehydrated with different concentrations of ethanol (30%, 50%, 70% and 80%), and then dehydrated with different concentrations of acetone (90%, 95% and 100%). The dehydrated specimens were placed in a mixture of acetone and Spurr resin (1: 1, V/V) for 1 hr, and transferred to a mixture of acetone and Spurr resin (1: 3, V/V) for 3 hr, then stored in Spurr resin overnight. Subsequently, the specimens were placed in Eppendorf containing Spurr resin and heated at 70°C for 9 hr. The heated specimens were sectioned with LEICA EM UC7 ultratome and the sections were stained with uranyl acetate and alkaline lead citrate for 5 min and 10 min, respectively. Finally, the stained specimens were observed with TEM.

1.5. *RNA extraction and RNA-Seq data analysis*

To compare the expression regulations effected by acid stress, four treatment samples were prepared for transcription analysis, including log phase sample (LP): log phase with $OD_{600} = 1.2$; persistent sample (PER): the log-phase culture was induced with acid for 7 days; recovery sample (RE): the log-phase culture was induced 20 days until no culturability and then resuspended in neutral LB for 48 hr until its OD_{600} start rising; recovery later sample (REL): the resuspension is incubated for another 12 hr with obvious OD_{600} rise (around 1.6 in three replicates). Each of the treatments was in three biological replicates.

The processes of cDNA construction and data generation are presented in Appendix A Text S1. The data generated from Illumina platform were used for bioinformatic analyses at the free online platform of Majorbio Cloud Platform (www.majorbio.com) from Shanghai Majorbio Bio-pharm Technology Co.,Ltd., China. The processes include data cleaning, mapping reads to reference genome, rRNA contamination assessment, expression analysis, differential expression analysis, DEGs GO enrichment analysis, DEGs KEGG enrichment analysis. The more detailed analysis procedure is referred to previous publications (Zhang et al., 2021; Wang et al., 2020).

1.6. *Determination of biphenyl and polychlorinated biphenyl (PCB) degradation efficiency*

TG9 was cultivated in LB until log phase, then the cells were resuspended to the same volume of inorganic salt solution. The cell resuspensions were set at pH 3, pH 5, pH 7 with HCl, and the control was set at pH 7 without TG9 inoculated, each set included 3 biological replicates. Meanwhile, 1 mL biphenyl solution with a concentration of 2500 mg/L was added to each of 12 glass centrifuge tubes, after the solvent hexane volatilized, 5 mL of each of the TG9 suspensions and the control was distributed to the 12 glass tubes to determine the degradation efficiency of biphenyl by TG9 at different pH. The initial nominal concentration of biphenyl is 500 mg/L in each of the tube. All of the tubes were cultured in a shaker set at 30°C and 180 r/min for 5 days, and then the residual biphenyl was extracted and determined to calculate its degradation amount by TG9 at different pH. The operating processes for PCB31 degradation are as same as biphenyl, but the degradation duration is 3 days. The calculation of the degradation efficiency: $(R_{con} - R_{tre}) / R_{con} \times 100\%$, R_{con}: residual in the control samples, R_{tre}: residual in the treatment samples. The detection methods of biphenyl and PCB 31 are described in Appendix A Text S1.

1.7. *Real-time reverse transcription quantitative PCR (RT-qPCR)*

Four groups of TG9 samples were prepared for RT-qPCR analyses, the control (OD_{600} =1.2 without acidification treatment), 24-hr acidification treatment, 48-hr acidification treatment

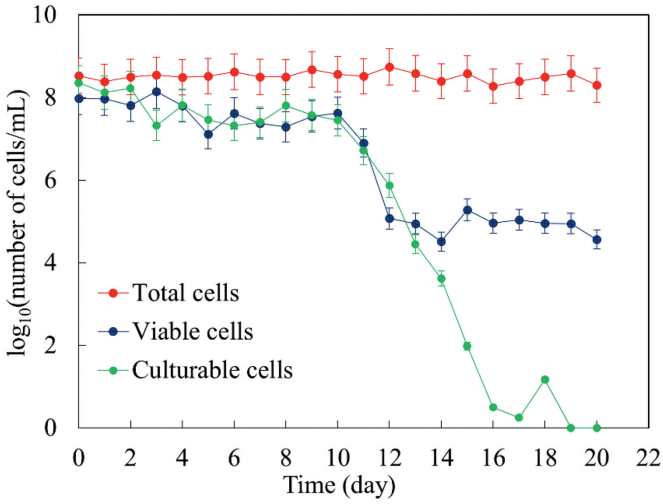

Fig. 1 – Variations of the number of total cells, viable cells and culturable cells under acid stress. The error bars in the figure represent 95% confidence intervals of the mean number of the counted cells (n = 4 including 4 biological replicates).

and 72-hr acidification treatment. Each of the treatments include 4 biological replicates. Depending on the transcriptome results, 8 genes were selected to further verify the expression regulations under acid stress in TG9, including *clpB, clpC, mrx1, mshA, pheA2, ogt, mmpL3* and *gadB*. In addition, 16S rRNA gene was selected as an internal reference. The primers of the 9 genes were designed with Primer-BLAST in NCBI, and their amplification efficiency was examined using both gel electrophoresis and RT-qPCR. The primer sequences were presented in Appendix A Table S1.

RNA from each sample was extracted with RNeasy Plus Mini Kit (QIAGEN, USA) based on the protocol provided by the manufacturer. The extracted RNA was immediately transcribed to cDNA with the mix of 6 μL PrimeScript^{TM} RT Master Mix (TaKaRa, USA), total RNA and 15 μL RNase Free dH_2O under the reaction condition 37°C for15 min and then 85°C for 5 sec. Subsequently, qPCR was conducted with 25 μL mix of 12.5 μL TB Green® Premix Ex Taq^{TM} II (TaKaRa, USA), 1 μL of each primers (10 μmol/L), 2 μL cDNA and 8.5 μL ddH_2O. The amplification was performed using the instrument BIO-RAD CFX96 touch qPCR system (USA) with the program 95°C for 3 min, 44 cycles of 95°C for 15 sec, 53°C for 20 sec and 72°C for 30 sec, and then melt curve of 65°C to 95°C. Each of the cDNA samples was amplified with three technical replicates. The fold change of the gene expression was calculated with the method of $2^{\wedge-\Delta\Delta CT}$.

2. Results and discussion

2.1. *Cell viability and culturability*

Under acid conditions, the number of the total cells maintains stable with more than 10^8 cells/mL (Fig. 1), suggesting that acidification suppressed cell division but not lysed the cells. Differently, the number of the culturable cells decreases slightly within the first 10 days and then decreases linearly afterwards until the detection limit (1 CFU/2 mL), except a sudden jump on day 18 (the reason for the jump is unclear). The number of the viable cells is somewhat consistent with that of the culturable cells in the first 12 days, but it remains rather constant with around 10^5 cells/mL afterwards. According to the reaction mechanism of CTC stain (Rodriguez et al., 1992), it suggests that part of the unculturable cell still have certain respiration. More than 10 days of culturability and viability indicate that TG9 possesses a strong capacity to resist and tolerate the acid stress, compared to other species which can only survive in such acid stress within hours, such as *Rhodococcus equi* (Benoit et al., 2000), *Lactobacillus* (Corcoran et al., 2005; Zhai et al., 2014), *Escherichia coli* (Ju et al., 2016). This rather long-term survival suggests that TG9 is able to adapt acid stress, which is conducive to contaminant detoxification and environmental remediation.

2.2. *Intracellular ATP concentration*

The intracellular ATP concentrations increase dramatically from 0.54 to 1.55 nm/mL on day 2 of acid induction (all the 12 values from 4 biological replicates × 3 technical replicates present the leap), but it then typically decreases to its quantification limit after day 13 (Fig. 2). Since ATP synthesis is activated by proton motive force which partly depends on proton gradient (Devaux et al., 2019), the sharp increase of the ATP concentration at 2-day acid treatment probably suggests that there was an increased proton gradient across the cell membrane under acid stress. In addition, the different trends between the numbers of the viable and culturable cells and the ATP concentrations within the first 10 days suggests that a high number of cells can retain culturability and viability with considerably low ATP concentration. Since ATP concentration is almost related to all physiological metabolisms in a cell, its low concentration suggests that TG9 possesses a global regulation ability to survive against ambient stresses. This might be one reason that TG9 can maintain the rather long-term culturability and viability under acid stress, and also under an-

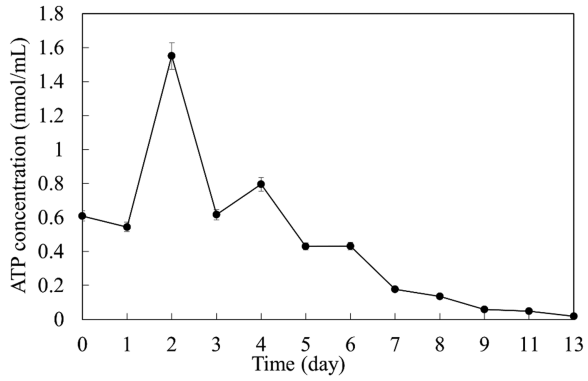

Fig. 2 – Concentration variations of the intracellular ATP in TG9 under acid stress. The unit in the y axis means nmol ATP per mL culture volume. The error bars represent 95% confidence intervals of the mean concentration of ATP ($n = 4$ including 4 biological replicates).

tibiotic stress (Jia et al., 2020) and oxygen deficit (Fan et al., 2021).

2.3. *Cell morphology*

The normal live cells are plump (Fig. 3a) and their intracellular materials distribute homogeneously (Fig. 3c). In contrast, the individual acid-induced cells shrink as a whole and are umbilicate, and the cell wall tethered tightly with cell membrane (Fig. 3b), which is different from normal dead cells with obvious winkle and separation between cell membrane and cell wall (labelled with white arrow in Fig. 3a). Meanwhile, the intracellular materials in acid-induced cells display visible aggregation and redistribution around the membrane (Fig. 3d). It has been found that some proteins can move and relocalize in response to metabolic and environmental triggers (Chong et al., 2015; Aimon et al., 2014). For instance, in *Escherichia coli*, more than half fraction of glutamate decarboxylase moves and relocates close to membrane when the pH in its medium falls to acidic condition (Capitani et al., 2003). In addition, the cells only shrunk but not lysed can support the observations of the constant number of total cells in Fig. 1.

2.4. *Degradation efficiency of organics*

Since TG9 is capable in degrading PCBs and biphenyl with a series of Bph enzymes (Ye et al., 2020), while its degradation efficiency could be impaired by acid stress. Here, the degradation of biphenyl and PCB31 was determined to assess the acid effects on the compound metabolism in TG9 (Fig. 4). The degradation efficiency is considerably weakened by acid stress at pH 3, especially for PCB31. In contrast, the degradation of PCB31 at pH 5 is similar as that at pH 7, but the efficiency decreases to around 40% for the degradation of biphenyl. For the degradation recession at acid pH, the explanation should be that there is a slightly decreased number of culturable cells (Fig. 1) and also the decreased ATP concentrations (Fig. 2) within the first 5 days. Taken together, TG9 has the capacity for PCB31 degradation at pH 5, but it is not so effective for biphenyl. Therefore, in the extremely acidified media, acid amelioration should be the first step before contamination bioremediation, and TG9 is still a potential strain for PCBs and biphenyl degradation in neutral and weak acid environmental compartments.

2.5. *Overview on regulation of gene expression*

The comparisons PER/LP, PER/RE were calculated to investigate the acid effects on the gene expressions compared to that in log phase and early recovery, and RE/LP, REL/LP illustrate the gene regulations in early recovery and late recovery referred to that in log phase, respectively. The genes with significant regulations are plotted to present a general view on expression changes among the four treatment samples in 14 main metabolism pathways (Fig. 5). It is obvious that the number of the upregulated genes in PER/LP are more than that in PER/RE in most of the pathways, but the number of the downregulated genes show the opposite difference (Fig. 5a). It indicates that after removing acid stress (RE) gene expressions become more active than that in log phase, which is also directly described by the comparisons of RE/LP that there are noticeably more upregulated genes than downregulated ones (Fig. 5b). This could, to some extent, elicit that the metabolism is more active after the recovery from acid stress, which may explain some observations that environmental stresses can enhance microorganisms resistance and survival in subsequent exposure to stimuli (Yuan et al., 2018; Mok and Brynildsen, 2018; He et al., 2016). However, the enhancement seems not last longer, since there are more genes downregulated in the comparisons of REL/LP than RE/LP. In addition, it is noticeable that the number of genes in translation pathway show more with downregulated expression than the upregulated ones in both of the comparisons PER/LP and PER/RE, indicating that acid stress repressed protein translation. In conclusion, TG9 can recover from unculturable state and had even higher gene expressions after the stress, suggesting that acidification induced a certain number of the cells in dormancy. The strong survivability of TG9 provides more potential to use it as an environmental remediation strain in the area polluted with both acid and other contaminants. The raw data on the transcription analysis is available in NCBI website with the accessing link https://www.ncbi.nlm.nih.gov/sra/PRJNA782447.

2.6. *Mechanism of metabolism response*

The large number of genes present significant regulated expressions explained above, which should correspond to certain metabolism tolerance and resistance to acid stress in TG9. In this part, the metabolism responses are interpreted from two directions. One is on the pathways containing the genes with extremely upregulated expressions in the comparisons PER/LP and PER/RE ($\log_2$(FC) $>$ 4) (FC: fold change of expression level between two treatments), including protein disaggregation and refolding, protein glycosylation, antioxidation, antipermeability of cell membrane and shikimate pathway. Another one is focused on proton consumption, neutralization and extrusion, including glutamate decarboxylation and glutamine deamidation, urea degradation, arginine deamination and oxidative phosphorylation. The processes with 95 genes involved are dissected in the following text and the mechanism model is built based on

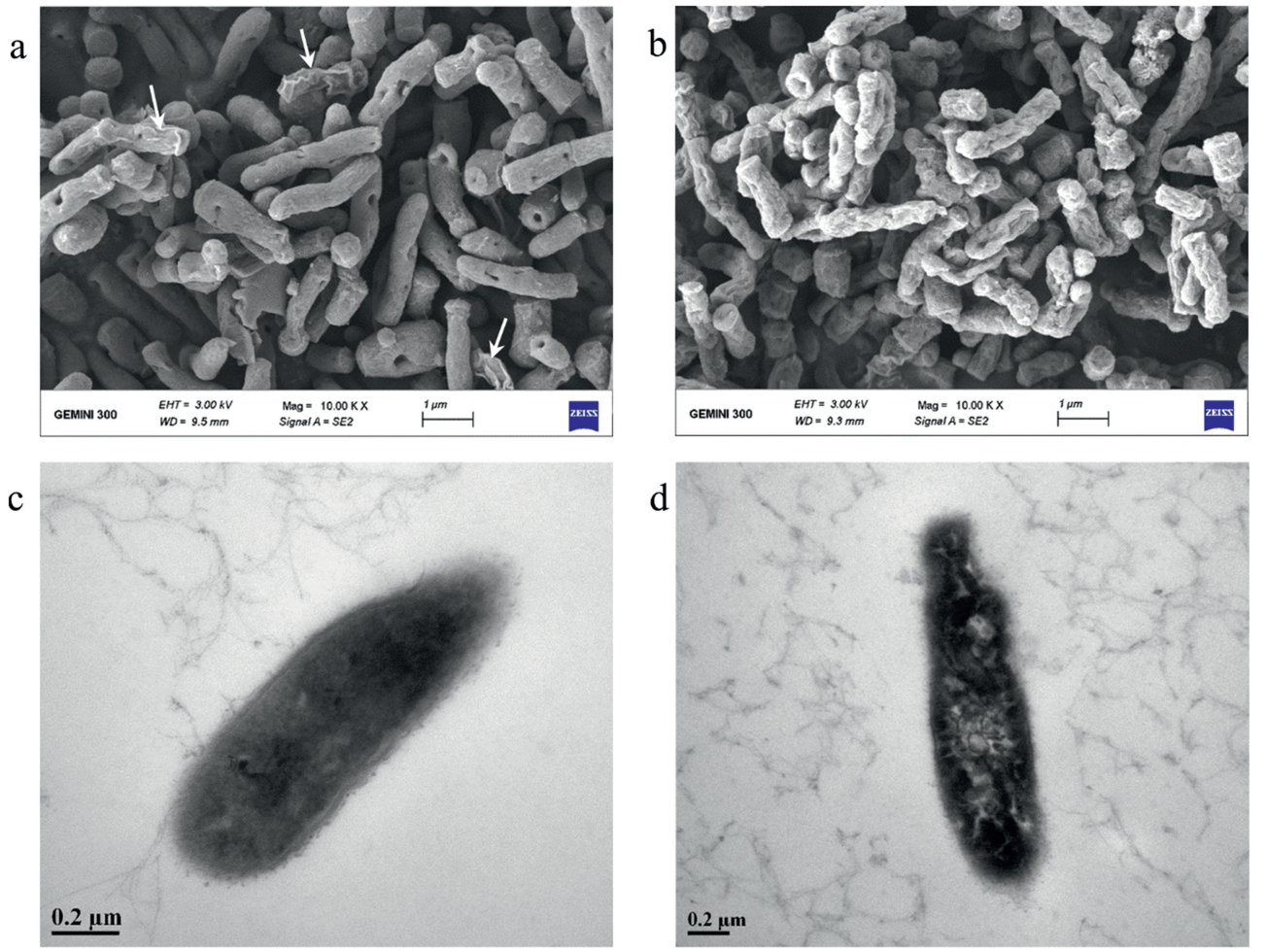

Fig. 3 – Morphology alterations of TG9 cells observed with SEM (a, b) and TEM (c, d), log phase sample (a and c), acid-induced sample which was induced at pH 3 until without culturability on day 19 (b and d). The white arrows in Fig. 3a label the dead cells in normal log phase.

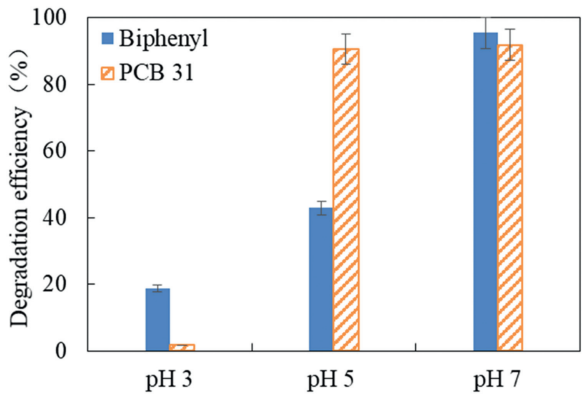

Fig. 4 – Degradation efficiency of biphenyl for 5 days and polychlorinated biphenyl (PCB) 31 for 3 days by TG9 at pH 3, pH 5 and pH 7. The error bars represent 95% confidence intervals of the mean degradation efficiency ($n = 3$ biological replicates), and the efficiency was calculated based on the residue of biphenyl or PCB31 in treated samples and control samples.

the interpretation of the metabolism responses (Appendix A Fig. S1).

Protein quality is predominantly controlled by several clusters of genes encoding adaptor proteins, protease and peptidase for protein disaggregation and refolding, which have been observed in many bacteria such as *Bacillus subtilis, Mycobacterium tuberculosis, Staphylococcus aureus, Escherichia coli* (Handtke, 2019; Springer et al., 2016; Battesti and Gottesman, 2013). To date, the processes have been frequently studied on genes *clpB, dnaK, grpE* and *dnaJ* (Zolkiewski, 1999; Lupoli et al., 2016; Mogk et al., 1999;) and genes *clpC* and *clpP* (Kirstein et al., 2007; Mashruwala et al., 2019). In TG9, both of the two groups of genes present significant upregulated expressions in the PER compared to that in the LP and Re, especially the genes *clpB* and *clpC* with $\log_2(FC) > 4$ (Appendix A Fig. S2a). Therefore, it indicates that the acid stress could result in protein aggregation in TG9, which is also proved by the heterogeneous entocyte observed in the TEM image (Fig. 3d), and the two disaggregation systems might strengthen its survival under acid stresses.

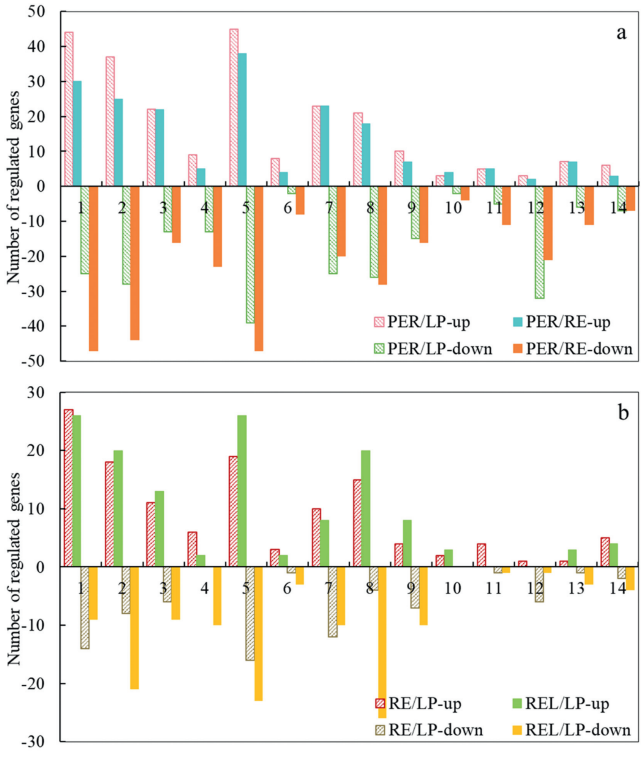

Fig. 5 – The number of genes with significant upregulated and downregulated expressions in 14 metabolism pathways enriched with KEGG pathway database. The figure (a) the comparisons PER/LP and PER/RE, and figure (b) presents RE/LP and REL/LP, respectively. The *x* axis is the numbered metabolism pathways, and the *y* axis is the number of upregulated (positive value) and downregulated (negative value) genes.

The gene *ogt* encoding *O*-linked *ß-N*-acetylglucosamine transferase (OGT) is responsible for the post-translational modification of numerous proteins, modulating signal transductions and transcriptional regulations in protecting cells against kinds of stresses such as heat shock, oxidation, high salinity, hypertonicity and toxicity in almost all organisms (Hart et al., 2011; Urso et al., 2020; Zachara et al., 2004; Liu et al., 2020). It was also found that *ogt* mutant or addition of OGT inhibitor can result in the arrest of growth or even cell lethality (Ostrowski et al., 2015; Wang et al., 2016). Therefore, the critical functions of OGT in protein modification should be the reason that the expression of *ogt* has dramatically higher regulations in the PER/LP and PER/RE (Appendix A Fig. S2a).

It is intriguing that the increase of glycosylation with OGT in cells can inhibit proteolytic degradation by inhibiting proteasomal ATPase activity (Zhang et al., 2003; Kudlow, 2006; Zachara and Hart, 2004). As a result, there should be a somewhat negative correlation between the expression variations of *ogt* gene and proteasomal genes (*pafA, dop, pup, prcA/B* and *arc*) in cells (Appendix A Fig. S1). In TG9, there is an intact pupylation-proteasomal gene group for post-translational modifications, but all of them typically show nonsignificant regulated expressions in the comparisons PER/LP and PER/RE (Appendix A Fig. S2a), which, to some extent, could be attributed to the inhibition by OGT.

TG9 has a complete group of genes required in MSH (mycothiol)/Mtr (mycothiol disulfide reductase)/NADPH (nicotinamide adenine dinucleotide phosphate) electron pathway, that is, it utilizes MSH as a reactive thiol and mycoredoxin 1 (Mrx1) as an antioxidant (Newton et al., 1996; Laer et al., 2012). This pathway is responsible for defending against oxidative damage from reactive oxygen species (ROS) (Appendix A Fig. S1) (Si et al., 2016; Hugo et al., 2014). The genes *mrx1* and *mtr* present significantly higher expressions in the PER/LP and PER/RE, while the expressions of genes *mshA, mshB, mshC* and *mshD* encoding for MSH synthesis show nonsignificant regulations or significant downregulations (Appendix A Fig. S2a). It means that the ROS reduction system could be disturbed by the lack of MSH to reduce oxidized Mrx1and then threaten TG9 survival.

The one possible explanation for the not upregulated expressions of the four msh genes can be that there is a competition in the substrate Uridine diphosphate *N*-acetylglucosamine (UDP-GlcNAc) between OGT and glycotransferase MshA (Appendix A Fig. S1). The MshA dedicatedly catalyzes UDP-GlcNAc with 1-L-myo-inositol-1-phosphate (1-L-Ins-1-P) to generate 3-phospho-1-D-myo-inosityl-2-acetamido-2-deoxy-α-D-glucopyranoside (GlcNAc-Ins-P) which is then used by MshB for the subsequent synthesis of MSH (Newton et al., 2006; Guo et al., 2017). Meanwhile, OGT transfers GlcNAc onto substrate proteins using UDP-GlcNAc as an obligate sugar donor (Dorfmueller et al., 2011; Nothaft and Szymanski, 2019). As mentioned above, the gene *ogt* encoding OGT presents significantly higher expressions in the PER/LP and PER/RE, suggesting that a higher amount of UDP-GlcNAc is consumed by OGT during protein glycosylation. As a consequence, the depletion of UDP-GlcNAc suppresses the synthesis of GlcNAc-Ins-P by MshA, resulting in the four genes *mshA, mshB, mshC* and *mshD* not as the other two genes mrx1 and mtr with significant upregulations. In addition, another factor which could also limit the expressions of *msh* genes is that the syntheses of 1-L-Ins-1-P and UDP-GlcNAc use the same substrate glucose 6-phosphate (Glc-6P) (Morii et al., 2018; Slawson et al., 2010). It suggests that the depletion of Glc-6P for UDP-GlcNAc synthesis could lower its availability for 1-L-Ins-1-P synthesis, and then suppresses the MshA activity. Taken together, it can be concluded the increasing protein glycosylation by OGT might inhibit MSH synthesis and then impairs the reducing capacity in TG9.

The shikimate pathway is responsible for the biosynthesis of three aromatic amino acids, vitamins and quinones in microorganisms, fungi and plants (Gibson and Pittard, 1968; Roberts et al., 2002). There are a series of enzymes involved in this pathway in TG9, except the gene *pheA2* ($\log_2$(FC) > 4), all the other genes (*aroF, aroB, aroD, aroQ, aroE, aroK, aroA, aroC, pheA1, tryA2* and *hisC*) present significant downregulated or nonsignificant regulated expressions in the PER/LP and PER/RE (Appendix A Fig. S2b). The first enzyme, 3-deoxy-

D-arabino-heptulosonate-7-phosphate synthase (DAHPS) encoded by gene *aro*F plays a crucial function as initiating the syntheses (Mir et al., 2015) (Appendix A Fig. S1). However, it has been examined that the primary intermediate, prephenate can inhibit more than 90% of DAHPS activity (Wu et al., 2005; Wu and Woodard, 2006). In the pathway, the enzymes prephenate dehydratase and prephenate dehydrogenase encoded by the genes *pheA2* and *tryA2* use prephenate as a substrate for the synthesis of phenylalanine and tyrosine, respectively. Nevertheless, it has been found that acid condition is more favorable for the activity of prephenate dehydratase rather than that of prephenate dehydrogenase (Hagino and Nakayama, 1974; Friedrich et al., 1976). Regarding this, one explanation for the dramatic expression of *pheA2* in the PER could be that TG9 tended to consume prephenate with prephenate dehydratase and reduce prephenate inhibition on DAHPS activity. Furthermore, by knockout of gene *pheA2*, it was found that prephenate dehydratase is involved in biofilm formation and stress tolerance including osmotic stress in *Acidovorax citrulli* (Kim et al., 2020). If it is so in TG9, then the high expression of *pheA2* should mainly work for the tolerance of acid stress.

The protein MmpL3 located in the inner membrane belongs to mycobacterial membrane protein Large transporter family. It plays an critical role in flipping trehalose monomycolates (TMM) across inner membrane to form mycolyl arabinogalactan-peptidoglycan (mAGP) complex which tethers the outer membrane to the cell wall (Xu et al., 2017; Su et al., 2019). This process can increase cell membrane rigidity and repress permeability of many compounds, that is why MmpL3 is an essential target of many antimicrobials (Li et al., 2014; Sethiya et al., 2020). In this study, gene *mmpL3* expressed significantly higher in the PER/LP and PER/RE with $\log_2$(FC) equaling 4.3 and 3.7, respectively (Appendix A Fig. S2a). That might be the reason that there is no visible separation between cell membrane and cell wall with acid treatment (Fig. 3b and d). Therefore, the upregulated expression of *mmpL3* should play an indispensable role in maintaining TG9 survival by repressing H^+ permeability under acid stress.

In glutamate metabolism, H^+ can be neutralized by ammonia via glutamine deamidation or be consumed via glutamate decarboxylation (Appendix A Fig. S1), and both of the reactions tend to be active in acid conditions (Lim et al., 2017; Cui et al., 2020; Teixeira et al., 2014). However, only the gene *gadB* encoding enzyme GadB for glutamate decarboxylation show significant upregulation, but the gene *glsA* encoding glutaminase for glutamine deamidation presents nonsignificant regulations in the PER/LP and PER/RE (Appendix A Fig. S2a). It suggests that the intracellular H^+ is more consumed by glutamate decarboxylation rather than glutamine deamidation. In addition, the upregulation of *gadB* with $\log_2$(FC) is slightly higher than 1, which might be limited by glutamate transport using glutamate transferase encoded by genes *gluA, gluB, gluC* and *gluD* with the nonsignificant or significant downregulated expressions. In line with the H^+ neutralization by ammonia, arginine deamination is another pathway to buffer the intracellular acid stress, the gene *arcA* encoding deaminase present significant upregulation in PER/LP (Appendix A Fig. S2b). Therefore, the arginine deamination can somewhat neutralize the excessive intracellular H^+. Meanwhile, urea degradation is another pathway that can produce ammonia to neutralize H^+ in cytoplasm (Appendix A Fig. S1), but the genes involved in this pathway present significant downregulations or nonsignificant regulations (Appendix A Fig. S2b). It indicates that urea degradation is not the main pathway for intracellular H^+ neutralization in TG9.

Besides the H^+ consumption and neutralization mentioned above, oxidative phosphorylation is another pathway directly influenced by acid stress, in which ATP is formed due to proton-motive force (Hatefi, 1985). In TG9, there are 39 genes involved in this metabolic process from the electron transport chain (complex I to IV) to ATP synthesis/hydrolysis (complex V) (Appendix A Fig. S1), while they have inconsistent expression regulations under acid stress (Appendix A Fig. S2c). The gene expressions in the subunits of complex I present significant upregulations or nonsignificant regulations, suggesting that the activity of complex I somewhat increased and the electron transport chain was initiated. However, the genes encoding the enzymes for complex II, III and IV show significant down-regulated or nonsignificant regulated expressions. This means that the acid stress somewhat blocked the electron transport chain from complex II to IV. It has been proved that the interrupt of electron transport chain can result in the dramatic release of ROS and consequently cause irreversible damage to DNA and cell structures (Dröse et al., 2016; Dröse and Brandt, 2008; Song et al., 2018). This can somehow potentially illustrate the reason that the gene *mrx1* encoding antioxidant mycoredoxin 1 in the MSH/Mtr/NADPH pathway has dramatically upregulated expression in the PER/LP and PER/RE.

The complex V, F_0F_1 ATP synthase in TG9 consists of 8 subunits including F_0 enzymes AtpB (a), AtpF (b) and AtpE (c) and F_1 enzymes AtpA (α), AtpD (ß), AtpG (γ), AtpC (ε) and AtpH (δ) (Appendix A Fig. S1). The F_0 subunits mainly function as proton transport and translocation, while the F_1 subunits are finally responsible for ATP synthesis and hydrolysis, especially the subunits ß, γ, ε are the dominant enzymes (Gao et al., 2005; Bianchet et al., 1998; Feniouk et al., 2006). The genes encoding the F_0 subunits present significant downregulations in the PER/LP and PER/RE, while the genes encoding the F_1 present significant upregulations or nonsignificant regulations (Appendix A Fig. S2c). Combining the inconsistent expression regulation of the genes in electron transport chain and the decreased expressions in F_0 subunits, it suggests that the proton transport was somewhat blocked by acid stress. Additionally, the rotation of subunit γ in F_1 sector is one of the main activities of ATP synthesis and hydrolysis, and F_0-induced γ rotation contributes to ATP synthesis while ATP-induced rotation is for ATP hydrolysis (Weber and Senior, 2000; Li et al., 2019). Therefore, the significantly downregulated expressions in F_0 subunits can certainly indicate that ATP synthesis is repressed in the PER. This can also be supported by that the ATP concentrations have noticeable decrease at day 7 (PER sampling time) compared with the initial value (LP sampling time) (Fig. 2). Meanwhile, the decreased ATP concentration suggests that ATP hydrolysis induced by ATP should also somewhat decrease. This can be further supported by that the genes *ppk2* and *ppk* encoding polyphosphate kinase and the gene *ppa* encoding inorganic diphosphatase have significant downregulated or nonsignificant regulated expressions (Appendix A Fig.

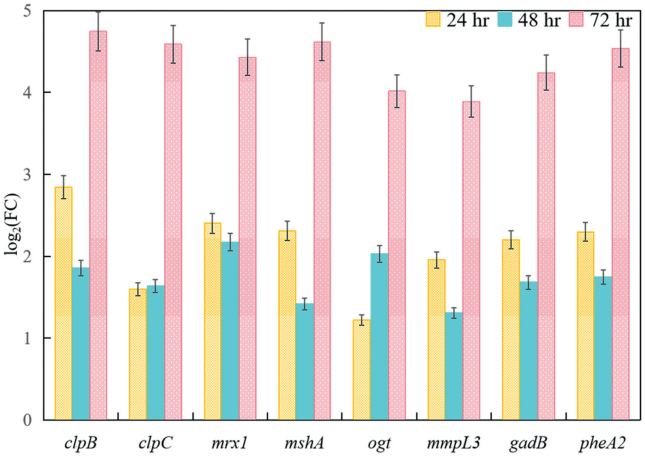

Fig. 6 – RT-qPCR validation of gene expression regulations. The *y* axis is the fold change (FC) of expression regulations and the *x* axis is the 8 genes selected. The error bars represent 95% confidence intervals of the mean $\log_2$(FC), $n = 4$ including 4 biological replicates, FC is calculated with $2^{-\Delta\Delta CT}$. The legend 24 hr, 48 hr and 72 hr expresses the gene regulations with 24-hr, 48-hr and 72-hr acidification treatment compared to the log phase ($OD_{600} = 1.2$) without acidification.

S2c). Furthermore, it has been found out that the subunit ε primarily functions as inhibition of ATP synthase, especially hydrolysis activity (Feniouk et al., 2006; Kato-yamada et al., 1999; Sielaff et al., 2018) and its expression is considerably upregulated with $\log_2$(FC) around 2 in the PER/LP and PER/RE. This implies that TG9 strived to inhibit the ATP hydrolysis and efficiently utilize its energy for survival under acid stress.

Consequently, the transcription results were interpreted on 10 metabolism pathways directly or generally related to acid stress, which suggests that TG9 possesses the ability to repair the damage and also to relieve the threat from acid stress. This comprehensive response system should be the primary reason that TG9 can survive long time under acid stress and also recover after removing acid. According to the interpretation, some approaches could be directly employed to further increase TG9 survival and its environmental functions under acid stress. There is substrate competition between glycosylation and antioxidation pathways, so the addition of substrate Glc-6P might promote the metabolism in these two pathways. For example, it has been found that addition of glucose can increase the survival of *Lactobacilli rhamnosus* under acid stress (Corcoran et al., 2005). In addition, since glutamate decarboxylation can consume H^+ and arginine deamination can neutralize H^+ with NH_3, the addition glutamate or arginine could also be a simple strategy to strengthen the tolerance and resistance of TG9 under acid stress. This has been proved in *E. coli* (Richard and Foster, 2004).

2.7. *Transcription validation with RT-qPCR*

The 8 genes *clpB, clpC, mrx1, mshA, ogt, mmpL3, gadB* and *pheA2* were selected for RT-qPCR analyses, located in the pathways of protein disaggregation and refolding, antioxidation, protein glycosylation, membrane stabilization and antipermeability, glutamate decarboxylation, shikimate pathway (Appendix A Fig. S1). Since these genes have extremely high upregulations in transcriptome analyses, except gene *mshA* does not regulate significantly but connects protein glycosylation and antioxidation, their transcription regulations were verified with 24-hr, 48-hr and 72-hr acidification treatments compared to the log phase without treatment (Fig. 6). From the RT-qPCR results, all the genes present significant upregulated expressions, especially at 72 hr, which are rather consistent with the transcriptome results. In addition, the transcription level of all the genes almost increase double at 72 hr compared to that at 24 and 48 hr, that might result from H^+ accumulation and stronger acid resistance in the cells with acidification duration.

Declaration of Competing Interest

The authors declare that they have no known competing financial interests or personal relationships that could have appeared to influence the work reported in this paper.

Acknowledgment

This work was supported by the National Key Research and Development Program of China (No. 2019YFC1803700), and the National Natural Science Foundation of China (Nos. 21876149 and 42077125). The authors would like to thank Bioultrastructure analysis Lab. of Analysis Center of Agrobiology and Environmental Sciences, Zhejiang University, China for helping in the electron microscopy analyses. Meanwhile, we are grateful for the help from our colleagues Assoc Prof. Jinsong Feng, MSc Li Guo, MSc Yunhan Jiang and MSc Zefan Liu.

Appendix A Supplementary data

Supplementary data associated with this article can be found in the online version at doi:10.1016/j.jes.2022.05.016.

REFERENCES

Aimon, S., Callan-Jones, A., Berthaud, A., Pinot, M., Toombes, G.E.S., Bassereau, P., 2014. Membrane shape modulates transmembrane protein distribution. Dev. Cell 28, 212–218.

Arya, S., Rautela, R., Chavan, D., Kumar, S., 2021. Evaluation of soil contamination due to crude E-waste recycling activities in the capital city of India. Process Saf. Environ. Prot. 152, 641–653.

Bang, M., Yong, C.-C., Ko, H.J., Choi, I.-G., Oh, S., 2018. Transcriptional response and enhanced intestinal adhesion ability of *Lactobacillus rhamnosus* GG after acid stress. J. Microbiol. Biotechnol. 28, 1604–1613.

Battesti, A., Gottesman, S., 2013. Roles of adaptor proteins in regulation of bacterial proteolysis. Curr. Opin. Microbiol. 16, 140–147.

Bell, K.S., Philp, J.C., Aw, D.W.J., Christofi, N., 1998. A review: the genus *Rhodococcus*. J. Appl. Microbiol. 85, 195–210.

Benoit, S., Benachour, A., Taouji, S., Auffray, Y., Hartke, A., 2001. Induction of *vap* genes encoded by the virulence plasmid of *Rhodococcus equi* during acid tolerance response. Res. Microbiol. 152, 439–449.

Benoit, S., Taouji, S., Benachour, A., Hartke, A., 2000. Resistance of *Rhodococcus equi* to acid pH. Int. J. Food. Microbiol. 55, 295–298.

Bianchet, M.A., Hullihen, J., Pedersen, P.L., Amzel, L.M., 1998. The 2.8-Å structure of rat liver F1-ATPase: configuration of a critical intermediate in ATP synthesis/hydrolysis. PNAS 95, 11065–11070.

Capitani, G., Biase, D.De, Aurizi, C., Gut, H., Bossa, F., Grutter, M.G., 2003. Crystal structure and functional analysis of *Escherichia coli* glutamate decarboxylase. EMBO J. 22, 4027–4037.

Carvalho, C.C.C.R.d., Fonseca, M.M.R.d., 2005. Degradation of hydrocarbons and alcohols at different temperatures and salinities by *Rhodococcus erythropolis* DCL14. FEMS Microbiol. Ecol. 51, 389–399.

Chakraborty, S., Winardhi, R.S., Morgan, L.K., Yan, J., Kenney, L.J., 2017. Non-canonical activation of OmpR drives acid and osmotic stress responses in single bacterial cells. Nat. Commun. 8, 1–14.

Chang, Y.-Y., Cronan, J.E., 1999. Membrane cyclopropane fatty acid content is a major factor in acid resistance of *Escherichia coli*. Mol. Microbiol. 33, 249–259.

Chong, Y.T., Koh, J.L.Y., Friesen, H., Duffy, K.S., Cox, M.J., Moses, A., et al., 2015. Yeast proteome dynamics from single cell imaging and automated analysis. Cell 161, 1413–1424.

Corcoran, B.M., Stanton, C., Fitzgerald, G.F., Ross, R.P., 2005. Survival of probiotic lactobacilli in acidic environments is enhanced in the presence of metabolizable sugars. Appl. Environ. Microbiol. 71, 3060–3067.

Cui, Y., Miao, K., Niyaphorn, S., Qu, X., 2020. Production of Gamma-aminobutyric acid from lactic acid bacteria: a systematic review. Int. J. Mol. Sci. 21, 1–21.

Devaux, J.B.L., Hedges, C.P., Birch, N., Herbert, N., Renshaw, G.M.C., Hickey, A.J.R., 2019. Acidosis maintains the function of brain mitochondria in hypoxia-tolerant triplefin fish: a strategy to survive acute hypoxic exposure? Front. Physiol. 9, 1–14.

Dobrowolski, R., Szcześ, A., Czemierska, M., Jarosz-Wikołazka, A., 2017. Studies of cadmium(II), lead(II), nickel(II), cobalt(II) and chromium(VI) sorption on extracellular polymeric substances produced by *Rhodococcus opacus* and *Rhodococcus rhodochrous*. Bioresour. Technol. 225, 113–120.

Domínguez-Ramírez, L.L., Rodríguez-Sanoja, R., Tecante, A., García-Garibay, M., Sainz, T., Wacher, C., 2020. Tolerance to acid and alkali by *Streptococcus infantarius* subsp. *infantarius* strain 25124 isolated from fermented nixtamal dough: Pozol. Studies in APT broth. Food Microbiol. 90, 1–9.

Doney, S.C., Busch, D.S., Cooley, S.R., Kroeker, K.J., 2020. The impacts of ocean acidification on marine ecosystems and reliant human communities. Annu. Rev. Environ. Resour. 45, 83–112.

Dorfmueller, H.C., Borodkin, V.S., Blair, D.E., Pathak, S., Navratilova, I., Aalten, D.M.F., 2011. Substrate and product analogues as human O-GlcNAc transferase inhibitors. Amino Acids 40, 781–792.

Dröse, S., Brandt, U., 2008. The mechanism of mitochondrial superoxide production by the cytochrome bc_1 complex. J. Biol. Chem. 283, 21649–21654.

Dröse, S., Stepanova, A., Galkin, A., 2016. Ischemic A/D transition of mitochondrial complex I and its role in ROS generation. Biochim. Biophys. Acta 1857, 946–957.

Edraki, M., Golding, S.D., Baublys, K.A., Lawrence, M.G., 2005. Hydrochemistry, mineralogy and sulfur isotope geochemistry of acid mine drainage at the Mt. Morgan mine environment, Queensland, Australia. Appl. Geochemistry 20, 789–805.

Fan, J., Jia, Y., Xu, D., Ye, Z., Zhou, J., Huang, J., et al., 2021. Anaerobic condition induces a viable but nonculturable state of the PCB-degrading bacteria *Rhodococcus biphenylivorans* TG9. Sci. Total Environ. 764, 1–8.

Favas, P.J.C., Sarkar, S.K., Rakshit, D., Venkatachalam, P., Prasad, M.N.V., 2016. Acid mine drainages from abandoned mines: hydrochemistry, environmental impact, resource recovery, and prevention of pollution. Environ. Mater. Waste 413–462.

Feng, S., Yang, H., Wang, W., 2015. System-level understanding of the potential acid-tolerance components of *Acidithiobacillus thiooxidans* ZJJN-3 under extreme acid stress. Extremophiles 19, 1029–1039.

Feniouk, B.A., Suzuki, T., Yoshida, M., 2006. The role of subunit epsilon in the catalysis and regulation of FOF1-ATP synthase. Biochim. Biophys. Acta 1757, 326–338.

Friedrich, C.G., Friedrich, B., Schlegel, H.G., 1976. Regulation of chorismate mutase prephenate dehydratase and prephenate dehydrogenase from *Alcaligenes eutrophus*. J. Bacteriol. 126, 723–732.

Gao, Y.Q., Yang, W., Karplus, M., 2005. A structure-based model for the synthesis and hydrolysis of ATP by F1-ATPase. Cell 123, 195–205.

Ge, X., Ma, S., Zhang, X., Yang, Y., Li, G., Yu, Y., 2020. Halogenated and organophosphorous flame retardants in surface soils from an e-waste dismantling park and its surrounding area: distributions, sources, and human health risks. Environ. Int. 139, 1–10.

Gibson, F., Pittard, J., 1968. Pathways of biosynthesis of aromatic amino acids and vitamins and their control in microorganisms. Bacteriol. Rev. 32, 465–492.

Guan, N., Liu, L., 2020. Microbial response to acid stress: mechanisms and applications. Appl. Microbiol. Biotechnol. 104, 51–65.

Guan, N., Shin, H., Chen, R.R., Li, J., Liu, L., Du, G., et al., 2014. Understanding of how *Propionibacterium acidipropionici* respond to propionic acid stress at the level of proteomics. Sci. Rep. 4, 1–8.

Guo, J.H., Liu, X.J., Zhang, Y., Shen, J.L., Han, W.X., Zhang, W.F., et al., 2010. Significant acidification in major Chinese croplands. Science 327, 1008–1010.

Guo, Y., Wang, L., Guo, J., Gu, G., Guo, Z., 2017. Biochemical studies of inositol N-acetylglucosaminyltransferase involved in mycothiol biosynthesis in *Corynebacterium diphtheria*. Org. Biomol. Chem. 15, 3775–3782.

Guo, Z.P., Khoomrung, S., Nielsen, J., Olsson, L., 2018. Changes in lipid metabolism convey acid tolerance in *Saccharomyces cerevisiae*. Biotechnol. Biofuels 11, 1–15.

Hagino, H., Nakayama, K., 1974. Regulatory properties of prephenate dehydrogenase and prephenate dehydratase from *Corynebacterium glutamicum*. Agric. Biol. Chem. 38, 2367–2376.

Handtke, I., 2019. Protein Quality Control and Antibiotics : the Role of the Small Heat Shock Protein YocM and the Disaggregase ClpC in B. subtilis. Protein Quality Control and Antibiotics : the Role of the Small Heat Shock Protein YocM and the Disaggregase ClpC in *B. subtilis*. Gottfried Wilhelm Leibniz Universität Hannover PhD. Thesis.

Hart, G.W., Slawson, C., Ramirez-correa, G., Lagerlof, O., 2011. Cross talk between O-GlcNAcylation and phosphorylation: roles in signaling, transcription, and chronic disease. Annu. Rev. Biochem. 80, 825–858.

Hatefi, Y., 1985. The mitchondrial electron transport and oxidative phosphorylation system. Ann. Rev. Biochem. 54, 1015–1069.

He, G., Wu, C., Huang, J., Zhou, R., 2016. Acid tolerance response of *Tetragenococcus halophilus*: a combined physiological and proteomic analysis. Process Biochem. 51, 213–219.

Hu, W., Feng, S., Tong, Y., Zhang, H., Yang, H., 2020. Adaptive defensive mechanism of bioleaching microorganisms under extremely environmental acid stress: advances and perspectives. Biotechnol. Adv. 42, 1–14.

Huang, X., Cui, Z., Ding, C., Su, Q., Lin, X., Wang, W., et al., 2021. Differential accumulation of short-, medium-, and long-chain chlorinated paraffin in free-range laying hens from an E-waste recycling area. J. Agric. Food Chem. 69, 10329–10337.

Hugo, M., Laer, K.Van, Reyes, A.M., Vertommen, D., Messens, J., Radi, R., et al., 2014. Mycothiol/mycoredoxin 1-dependent reduction of the peroxiredoxin AhpE from *Mycobacterium tuberculosis*. J. Biol. Chem. 289, 5228–5239.

Inoue, D., Nakazawa, M., Yamamoto, N., Sei, K., Ike, M., 2020. Draft genome sequence of *Rhodococcus aetherivorans* JCM 14343T, a bacterium capable of degrading recalcitrant noncyclic and cyclic ethers. Microbiol. Resour. Announc. 9, 1–2.

Jan, G., Leverrier, P., Pichereau, V., Boyaval, P., 2001. Changes in protein synthesis and morphology during acid adaptation of *Propionibacterium freudenreichii*. Appl. Environ. Microbiol. 67, 2029–2036.

Jia, Y., Yu, C., Fan, J., Fu, Y., Ye, Z., Guo, X., et al., 2020. Alterations in the cell wall of *Rhodococcus biphenylivorans* under norfloxacin stress. Front. Microbiol. 11, 1–10.

Jones, A.L., Goodfellow, M., 2015. *Rhodococcus*. Bergey's Man. syst. Archaea Bact. 1–50.

Ju, S.Y., Kim, J.H., Lee, P.C., 2016. Long-term adaptive evolution of *Leuconostoc mesenteroides* for enhancement of lactic acid tolerance and production. Biotechnol. Biofuels 9, 1–12.

Kato-yamada, Y., Bald, D., Koike, M., Motohashi, K., Hisabori, T., Yoshida, M., 1999. ε Subunit, an endogenous inhibitor of bacterial F1-ATPase, also inhibits F0F1-ATPase. J. Biol. Chem. 274, 33991–33994.

Kenney, L.J., 2019. The role of acid stress in *Salmonella* pathogenesis. Curr. Opin. Microbiol. 47, 45–51.

Kim, M., Lee, J., Heo, L., Han, S.W., 2020. Putative bifunctional chorismate mutase/prephenate dehydratase contributes to the virulence of *Acidovorax citrulli*. Front. Plant Sci. 11, 1–12.

Kirstein, J., Dougan, D.A., Gerth, U., Hecker, M., 2007. The tyrosine kinase McsB is a regulated adaptor protein for ClpCP. EMBO J. 26, 2061–2070.

Kudlow, J.E., 2006. Post-translational modification by O-GlcNAc: another way to change protein function. J. Cell Biochem. 98, 1062–1075.

Laer, K.V., Buts, L., Foloppe, N., Vertommen, D., Belle, K.V., Wahni, K., et al., 2012. Mycoredoxin-1 is one of the missing links in the oxidative stress defence mechanism of *Mycobacteria*. Mol. Microbiol. 86, 787–804.

LeBlanc, J.C., Gonçalves, E.R., Mohn, W.W., 2008. Global response to desiccation stress in the soil actinomycete *Rhodococcus jostii* RHA1. Appl. Environ. Microbiol. 74, 2627–2636.

Li, W., Upadhyay, A., Fontes, F.L., North, E.J., Wang, Y., Crans, D.C., et al., 2014. Novel insights into the mechanism of inhibition of MmpL3, a target of multiple pharmacophores in *Mycobacterium tuberculosis*. Antimicrob. Agents Chemother. 58, 6413–6423.

Li, Y., Ma, X., Weber, J., 2019. Interaction between γC87 and γR242 residues participates in energy coupling between catalysis and proton translocation in *Escherichia coli* ATP synthase. Biochim. Biophys. Acta-Bioenerg. 1860, 679–687.

Lim, H.S., Cha, I.T., Roh, S.W., Shin, H.H., Seo, M.J., 2017. Enhanced production of Gamma-aminobutyric acid by optimizing culture conditions of *Lactobacillus brevis* HYE1 isolated from Kimchi, a Korean Fermented Food. J. Microbiol. Biotechnol. 27, 450–459.

Lindberg, L., Santos, A.X.S., Riezman, H., Olsson, L., Bettiga, M., 2013. Lipidomic profiling of *Saccharomyces cerevisiae* and *Zygosaccharomyces bailii* reveals critical changes in lipid composition in response to acetic acid stress. PLoS ONE 8, 1–12.

Liu, Y., Tang, H., Lin, Z., Xu, P., 2015. Mechanisms of acid tolerance in bacteria and prospects in biotechnology and bioremediation. Biotechnol. Adv. 33, 1484–1492.

Liu, Y., Chen, Q., Zhang, N., Zhang, K., Dou, T., Cao, Y., et al., 2020. Proteomic profiling and genome-wide mapping of O-GlcNAc chromatin-associated proteins reveal an O-GlcNAc-regulated genotoxic stress response. Nat. Commun. 11, 1–17.

Lupoli, T.J., Fay, A., Adura, C., Glickman, M.S., Nathan, C.F., 2016. Reconstitution of a *Mycobacterium tuberculosis* proteostasis network highlights essential cofactor interactions with chaperone DnaK. PNAS 113, 7947–7956.

Lyu, C., Zhao, W., Peng, C., Hu, S., Fang, H., Hua, Y., et al., 2018. Exploring the contributions of two glutamate decarboxylase isozymes in *Lactobacillus brevis* to acid resistance and γ-aminobutyric acid production. Microb. Cell Fact. 17, 1–14.

Maass, D., Todescato, D., Moritz, D.E., Oliveira, J.V., Oliveira, D., Ulson De Souza, A.A., et al., 2015. Desulfurization and denitrogenation of heavy gas oil by *Rhodococcus erythropolis* ATCC 4277. Bioprocess Biosyst. Eng. 38, 1447–1453.

Mangold, S., Jonna, V.rao, Dopson, M., 2013. Response of *Acidithiobacillus caldus* toward suboptimal pH conditions. Extremophiles 17, 689–696.

Martins, F., Felgueiras, C., Smitkova, M., Caetano, N., 2019. Analysis of fossil fuel energy consumption and environmental impacts in European countries. Energies 12, 1–11.

Mashruwala, A.A., Eilers, B.J., Fuchs, A.L., Norambuena, J., Earle, C.A., Guchte, A., van de, et al., 2019. The ClpCP complex modulates respiratory metabolism in Staphylococcus aureus and is regulated in a SrrAB-dependent manner. J. Bacteriol. 201, 1–18.

Meng, C., Tian, D., Zeng, H., Li, Z., Yi, C., Niu, S., 2019. Global soil acidification impacts on belowground processes. Environ. Res. Lett. 14, 1–10.

Merrell, D.S., Camilli, A., 2002. Acid tolerance of gastrointestinal pathogens. Curr. Opin. Microbiol. 5, 51–55.

Mir, R., Jallu, S., Singh, T.P., 2015. The shikimate pathway: review of amino acid sequence, function and three-dimensional structures of the enzymes. Crit. Rev. Microbiol. 41, 172–189.

Mogk, A., Tomoyasu, T., Goloubinoff, P., Ruediger, S., Roeder, D., Langen, H., et al., 1999. Identification of thermolabile *Escherichia coli* proteins: prevention and reversion of aggregation by DnaK and ClpB. EMBO J. 18, 6934–6949.

Mok, W.W.K., Brynildsen, M.P., 2018. Timing of DNA damage responses impacts persistence to fluoroquinolones. PNAS 115, E6301–E6309.

Morii, H., Nishimura, T., Takeo, M., Katayama, C., Kakai, K., 2018. Preparation of 1L-myo-inositol 1-phosphate as a substrate of phosphatidylinositol phosphate synthase. J. UOEH 40, 217–224.

Newton, G.L., Arnold, K., Price, M.S., Sherrill, C., Delcardayre, S.B., Aharonowitz, Y., et al., 1996. Distribution of thiols in microorganisms: mycothiol is a major thiol in most *Actinomycetes*. J. Bacteriol. 178, 1990–1995.

Newton, G.L., Ta, P., Bzymek, K.P., Fahey, R.C., 2006. Biochemistry of the initial steps of mycothiol biosynthesis. J. Biol. Chem. 281, 33910–33920.

Nothaft, H., Szymanski, C.M., 2019. New discoveries in bacterial N-glycosylation to expand the synthetic biology toolbox. Curr. Opin. Chem. Biol. 53, 16–24.

Ostrowski, A., Gundogdu, M., Ferenbach, A.T., Lebedev, A.A., van Aalten, D.M.F., va, 2015. Evidence for a functional O-linked *N*-acetylglucosamine (O-GlcNAc) system in the thermophilic bacterium *Thermobaculum terrenum*. J. Biol. Chem. 290, 30291–30305.

Palma, M., Guerreiro, J.F., Sá-Correia, I., 2018. Adaptive response and tolerance to acetic acid in *Saccharomyces cerevisiae* and *Zygosaccharomyces bailii*: a physiological genomics perspective. Front. Microbiol. 9, 1–16.

Richard, H., Foster, J.W., 2004. Escherichia coli glutamate- and arginine-dependent acid resistance systems increase internal pH and reverse transmembrane potential. J. Bacteriol. 186, 6032–6041.

Roberts, C.W., Roberts, F., Lyons, R.E., Kirisits, M.J., Mui, E.J., Finnerty, J., et al., 2002. The shikimate pathway and its branches in apicomplexan parasites. J. Infect. Dis. 185, S25–S36.

Rodriguez, G.G., Phipps, D., Ishiguro, K., Ridgway, H.F., 1992. Use of a fluorescent redox probe for direct visualization of actively respiring bacteria. Appl. Environ. Microbiol. 58, 1801–1808.

Sethiya, J.P., Sowards, M.A., Jackson, M., North, E.J., 2020. MmpL3 inhibition: a new approach to treat nontuberculous mycobacterial infections. Int. J. Mol. Sci. 21, 1–25.

Shen, G., Zhang, S., Liu, X., Jiang, Q., Ding, W., 2018. Soil acidification amendments change the rhizosphere bacterial community of tobacco in a bacterial wilt affected field. Appl. Microbiol. Biotechnol. 102, 9781–9791.

Si, M., Zhao, C., Zhang, B., Wei, D., Chen, K., Yang, X., et al., 2016. Overexpression of mycothiol disulfide reductase enhances corynebacterium glutamicum robustness by modulating cellular redox homeostasis and antioxidant proteins under oxidative stress. Sci. Rep. 6, 1–14.

Sielaff, H., Duncan, T.M., Börsch, M., 2018. The regulatory subunit ε in *Escherichia coli* FOF1-ATP synthase. Biochim. Biophys. Acta-Bioenerg. 1859, 775–788.

Slawson, C., Copeland, R.J., Hart, G.W., 2010. O-GlcNAc signaling: a metabolic link between diabetes and cancer? Trends Biochem. Sci. 35, 547–555.

Sohlenkamp, C., 2017. Membrane homeostasis in bacteria upon pH Challenge. In: Geiger, O. (Ed.), Biogenesis of Fatty Acids, Lipids and Membranes. Handbook of Hydrocarbon and Lipid Microbiology. Springer, Cham, pp. 1–13.

Song, E., Ramos, S.V, Huang, X., Liu, Y., Botta, A., Sung, H.K., et al., 2018. Holo-lipocalin-2-derived siderophores increase mitochondrial ROS and impair oxidative phosphorylation in rat cardiomyocytes. PNAS 115, 1576–1581.

Springer, M.T., Singh, V.K., Cheung, A.L., Donegan, N.P., Chamberlain, N.R., 2016. Effect of *clpP* and *clpC* deletion on persister cell number in Staphylococcus aureus. J. Medi. Microb. 65, 848–857.

Su, C.C., Klenotic, P.A., Bolla, J.R., Purdy, G.E., Robinson, C.V., Yu, E.W., 2019. MmpL3 is a lipid transporter that binds trehalose monomycolate and phosphatidylethanolamine. PNAS 116, 11241–11246.

Su, X., Liu, Y., Hashmi, M.Z., Hu, J., Ding, L., Wu, M., et al., 2015. *Rhodococcus biphenylivorans* sp. nov., a polychlorinated biphenyl-degrading bacterium. Antonie van Leeuwenhoek, 107, 55–63.

Sun, Y., 2016. F1F0-ATPase functions under markedly acidic conditions in bacteria. Adv. Biochem. Health Dis. 14, 459–468.

Suyal, D.C., Joshi, D., Kumar, S., Soni, R., Goel, R., 2019. Differential protein profiling of soil diazotroph *Rhodococcus qingshengii* S10107 towards low-temperature and nitrogen deficiency. Sci. Rep. 9, 1–9.

Teixeira, J.S., Seeras, A., Sanchez-Maldonado, A.F., Zhang, C., Su, M.S.W., Gänzle, M.G., 2014. Glutamine, glutamate, and arginine-based acid resistance in *Lactobacillus reuteri*. Food Microbiol 42, 172–180.

Urso, S.J., Comly, M., Hanover, J.A., Lamitina, T., 2020. The O-GlcNAc transferase OGT is a conserved and essential regulator of the cellular and organismal response to hypertonic stress. Plos Genet. 16, 1–27.

Wang, A.C., Jensen, E.H., Rexach, J.E., Vinters, H.V., Hsieh-wilson, L.C., 2016. Loss of O-GlcNAc glycosylation in forebrain excitatory neurons induces neurodegeneration. PNAS 113, 15120–15125.

Wang, C., Chen, Y., Zhou, H., Li, X., Tan, Z., 2020. Adaptation mechanisms of *Rhodococcus sp.* CNS16 under different temperature gradients: physiological and transcriptome. Chemosphere 238, 1–11.

Weber, J., Senior, A.E., 2000. ATP synthase: what we know about ATP hydrolysis and what we do not know about ATP synthesis. Biochim. Biophys. Acta 1458, 300–309.

Wu, J., Sheflyan, G.Y., Woodard, R.W., 2005. *Bacillus subtilis* 3-deoxy-D-arabino-heptulosonate 7-phosphate synthase revisited: resolution of two long-standing enigmas. Biochem. J. 390, 583–590.

Wu, J., Woodard, R.W., 2006. New insights into the evolutionary links relating to the 3-Deoxy-D-arabino-heptulosonate 7-phosphate synthase subfamilies. J. Biol. Chem. 281, 4042–4048.

Xu, Z., Meshcheryakov, V.A., Poce, G., Chng, S.S., 2017. MmpL3 is the flippase for mycolic acids in mycobacteria. PNAS 114, 7993–7998.

Ye, Z., Li, H., Jia, Y., Fan, J., Wan, J., Guo, L., et al., 2020. Supplementing resuscitation - promoting factor (Rpf) enhanced biodegradation of polychlorinated biphenyls (PCBs) by *Rhodococcus biphenylivorans* strain TG9^T. Environ. Pollut. 263, 1–10.

Yuan, W., Seng, Z.J., Kohli, G.S., Yang, L., Yuk, H.G., 2018. Stress resistance development and genome-wide transcriptional response of *Escherichia coli* O157:H7 adapted to sublethal thymol, carvacrol, and trans-cinnamaldehyde. Appl. Environ. Microbiol. 84, 1–14.

Yun, Y., Wang, H., Man, B., Xiang, X., Zhou, J., Qiu, X., et al., 2016. The relationship between pH and bacterial communities in a single karst ecosystem and its implication for soil acidification. Front. Microbiol. 7, 23–32.

Zachara, N.E., Hart, G.W., 2004. O-GlcNAc modification: a nutritional sensor that modulates proteasome function. Trend Cell Biol. 14, 218–221.

Zachara, N.E., O'Donnell, N., Cheung, W.D., Mercer, J.J., Marth, J.D., Hart, G.W., 2004. Dynamic O-GlcNAc modification of nucleocytoplasmic proteins in response to stress. J. Biol. Chem. 279, 30133–30142.

Zhai, Z., Douillard, F.P., An, H., Wang, G., Guo, X., Luo, Y., et al., 2014. Proteomic characterization of the acid tolerance response in *Lactobacillus delbrueckii* subsp. bulgaricus CAUH1 and functional identification of a novel acid stress-related transcriptional regulator Ldb0677. Environ. Microbiol. 16, 1524–1537.

Zhang, F., Su, K., Yang, X., Bowe, D.B., Paterson, A.J., Kudlow, J.E., 2003. O-GlcNAc modification is an endogenous inhibitor of the proteasome. Cell 115, 715–725.

Zhang, X., Liu, W., Zhang, G., Jiang, L., Han, X., 2015. Mechanisms of soil acidification reducing bacterial diversity. Soil Biol. Biochem. 81, 275–281.

Zhang, X., Zhou, D., Bai, H., Liu, Q., Xiao, X.L., Yu, Y.G., 2021. Comparative transcriptome analysis of virulence genes of enterohemorrhagic *Escherichia coli* O157:H7 to acid stress. Food Biotechnol. 35, 91–110.

Zhang, Y., Zhang, Y., Xiong, J., Zhao, Z., Chai, T., 2019. The enhancement of pyridine degradation by *Rhodococcus* KDPy1 in coking wastewater. FEMS. Microbiol. Lett. 366, 1–7.

Zhou, C., Fey, P.D., 2020. The acid response network of *Staphylococcus aureus*. Curr. Opin. Microbiol. 55, 67–73.

Zhu, Z., Yang, J., Yang, P., Wu, Z., Zhang, J., Du, G., 2019. Enhanced acid-stress tolerance in *Lactococcus lactis* NZ9000 by overexpression of ABC transporters. Microb. Cell Fact. 18, 1–14.

Zolkiewski, M., 1999. ClpB cooperates with DnaK, DnaJ, and GrpE in suppressing protein aggregation. J. Biol. Chem. 274, 28083–28087.